JOURNAL OF AEROSPACE COMPUTING, INFORMATION, AND COMMUNICATION
Vol. 3, January 2006

Performance and Capacity of Direct-Sequence Spread Spectrum Overlay in the Microwave Landing System Band*,†

David W. Matolak and Joshua T. Neville
Ohio University, Athens, Ohio

We examine the performance of a direct-sequence spread spectrum (DS-SS) code-division multiple-access (CDMA) system used in a spectral overlay mode in the Microwave Landing System (MLS) band, from 5091–5150 MHz. The purpose of the overlay system is to enable increased spectral efficiency (higher data throughput), for future potential aeronautical datalink communications, particularly for short-range systems such as for airport surface, and terminal areas. We estimate the performance degradation incurred by both systems for a range of relative transmit powers, several DS-SS bandwidths and data rates, and example MLS and DS-SS system parameters, including the number of DS-SS users. We also briefly examine the use of multicarrier (MC) DS-SS signaling techniques. Our study uses both analysis and computer simulations, and complements prior work done for the use of DS-SS in the Instrument Landing System Glideslope band, where the ILS signal is an analog signal, in contrast to the (analog and) digital MLS signal. We provide examples that explore both MLS and DS-SS system parameter values appropriate for the successful application of overlay.

I. Introduction

ADDITIONAL communication capabilities in civilian aviation are widely cited as critical to continued efficient air travel. For example, the Federal Aviation Administration's (FAA) National Airspace System (NAS) "modernization blueprint",[1] any one of numerous papers from recent professional conferences in the field, such as the Digital Avionics Systems Conferences (DASC), e.g., Refs. 2, 3 or recent Integrated Communications, Navigation, and Surveillance (ICNS) workshops, e.g., Refs. 4, 5 can be cited to support this. Communication service growth for passenger communications is also expected.[6] In this work we present another study in the area of feasibility and tradeoff analyses aimed at exploring possible methods to provide new aviation communication services. Recent other works in this area, particularly on integrating communications, navigation, and surveillance (CNS), include.[7,8]

Traditionally, each component of the NAS has occupied and operated independently, in its own reserved frequency spectrum. For example, VHF communications is allocated the 118.0–137.0 MHz frequency spectrum, navigation is allocated 108–118 MHz, 329–335 MHz and parts of the band in the 900–1020 MHz spectrum (e.g., DME covers 978 MHz to 1213 MHz), and some surveillance (secondary radar transponders) is allocated 1030/1090 MHz plus guard bands. Next generation Air Traffic Control/Air Traffic Management (ATC/ATM) infrastructure development and systems, such as proposed by the NASA Small Aircraft Transportation System (SATS), are driving toward an

Received 4 August 2004; revision received 11 November 2004; accepted for publication 12 December 2005.

*A portion of this work was published in *Proc. IEEE Aerospace Conf.*, Session 4.18, Big Sky, MT, March 6–13, 2004, matolak@ohiou.edu

†This work was supported by the FAA, through NASA Glenn Research Center, NASA grant NAG3-2815, jn405297@ohio.edu

"integrated" CNS system solution that can operate in a single "swath" of spectrum to gain efficiency in bandwidth usage and economy from integration of services.

This work, in support of NASA Glenn and the FAA, is part of a study to explore innovative approaches to providing new communications services. We focus here on the Microwave Landing System (MLS) band, from 5091–5150 MHz. Based upon common (e.g., terrestrial cellular radio) versions of direct-sequence spread-spectrum (DS-SS) systems, we investigate the use of spectral overlay—the simultaneous use of DS-SS and a narrowband (MLS) system in the same band.[9,10] This concept relies on the interference suppression capabilities of DS-SS to enable higher aggregate throughputs than are possible with either a narrowband or DS-SS signaling scheme alone. Worth noting is that overlay is something of a worst-case for both systems, in that orthogonal (non-overlapping) spectral allocations would result in minimal inter-system interference, and consequently better performance for both.

We derive expressions for the performance of both the DS-SS and MLS systems in the presence of each other, for a range of relative transmit powers, several DS-SS bandwidths, data rates and numbers of users, and typical MLS and CDMA system parameters. We use both analysis and computer simulations. A similar study for the Instrument Landing System (ILS) Glideslope (GS) band, from 329–334 MHz, was recently completed.[11] In that case, the narrowband analog ILS-GS signal consists of multiple tones, whereas here, the MLS signal is a digitally-modulated signal as well as a spatially-swept tone. We employ classical analytical techniques, corroborated by computer simulation, to characterize the performance of both DS-SS and MLS systems in the presence of each other, under several assumptions described subsequently. In addition, since the MLS signal radiates from a ground site, our study considers specifically the ground to air (GA) uplink, or "forward" channel. Air to ground (AG) communications (the "reverse" channel) would generally be accomplished in a different frequency band (i.e., using frequency division duplex, FDD), and hence would incur little or no MLS interference other than out-of-band emissions, which are generally low if adequate physical separation and filtering are employed. In the GA setting, multiple DS-SS signals can be transmitted in synchronism, for a DS code-division multiple access (CDMA) scheme.

In Section II we describe the system model, assumptions, and introduce notation. The mathematical analysis of performance is in Section III, for both systems, and in Section IV we provide numerical results—both analytical and simulations. Section V contains a summary and conclusions.

II. System and Signal Models

We assume that the MLS signal has an arbitrary center frequency within the main spectral lobe of the DS-SS signal, i.e., $f_c - R_c \leq f_{c,M} \leq f_c + R_c$, where f_c is the DS-SS carrier frequency and R_c the DS-SS chip rate, and $f_{c,M}$ is the MLS carrier frequency. The condition $f_{c,M} = f_c$ is a worst case condition for the DS-SS receiver, and in fact, this case is simpler to evaluate than the general case. In addition, multipath is neglected to simplify analysis. For most applications, the aircraft will have a line of sight to the ground transceivers, hence, our first order model for the channel is an additive white Gaussian noise (AWGN) channel. Figure 1 shows our system conceptual model.

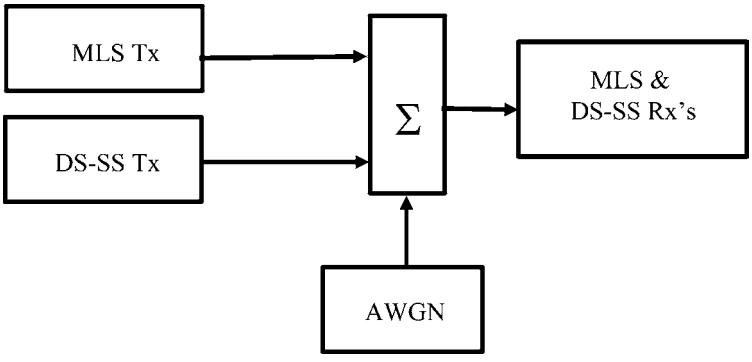

Fig. 1 Conceptual model of DS-SS overlay system. [From paper in *Proc. IEEE Aerospace Conf.* (March 6–13, 2004), © 2004 IEEE, Reprinted with permission.]

Extension of this work to dispersive channels is reasonably straightforward,[12] and may be an area for future work, as is additional work on the use of multicarrier (MC) schemes.[13]

The MLS system scans an antenna beam across a spatial angle centered on the runway,[14,15] and hence depending on the spatial location of the aircraft, the MLS signal would generally not be received continuously by a given aircraft (aloft or on the surface). The scanned signal is a single tone, separated in time from (following) the transmission of the MLS digital signal, which can contain information such as runway heading, airport identity, and glide path angle. For simplicity, in this work we focus only on the *digital* transmission portion of the MLS. Determination of the effect of the scanned MLS tone signal upon the DS-SS signal can be obtained from results obtained in other studies, e.g.[11,12]. A complete study of the effect of the MLS system upon a DS-SS signal would account for both the analog (tone) and digital portions of the MLS transmission, and also include the spatial effects of the antenna beam and relative aircraft location. We reserve this comprehensive study for future work, which would make use of results obtained both here and in[11]. Henceforth, when we refer to the MLS signal, we mean only the *digital* part of the MLS transmission.

The MLS signal is a narrowband differential binary phase-shift keying (DBPSK) signal, with a bit rate of $R_{bM} = 15.625$ kbps. It can be described as follows:

$$s_M(t) = \sqrt{2P_M} d_M(t) \cos(\omega_{c,M} t + \theta) \tag{1}$$

where P_M is the power in the MLS signal, and $d_M(t)$ is the data bearing signal. The carrier radian frequency is $\omega_{c,M} = 2\pi f_{c,M}$, and the carrier phase is θ. Equation (1) is with reference to the receiver(s). The MLS signal power $P_M = E_{bM} R_{bM}$, with $E_{bM} = E_M$ the energy per bit of the MLS signal. The MLS data signal is given by

$$d_M(t) = \sum_k d_{M,k} p_{T_M}(t - kT_M) \tag{2}$$

where $d_{M,k} \in \{\pm 1\}$ is the k^{th} bit, $T_M = 1/R_{bM}$ is the bit duration, and $p_x(t)$ is a unit amplitude rectangular pulse non-zero only in the interval *[0,x)*. The data bits are differentially-encoded, so that the actual k^{th} information bit $b_k \in \{0, 1\}$ is related to $d_{M,k}$ by $d_{M,k} = 2(\tilde{d}_{M,k-1} \oplus b_k) - 1$, where $\tilde{d}_{M,k-1}$ is the logical binary version of $d_{M,k-1}$, i.e., $\tilde{d}_{M,k-1} \in \{0, 1\}$, and $d_{M,k} = 2\tilde{d}_{M,k-1} - 1$, and the symbol $\oplus$ is the logical exclusive-OR.

We assume for simplicity that the DS-SS signal is binary phase modulated (BPSK), and also assume coherent detection. The single-carrier (SC) DS-SS signal received by the aircraft is defined similar to the MLS signal. For the k^{th} DS-SS user, we have

$$s_k(t) = \sqrt{2P_k} d_k(t) c_k(t) \cos(\omega_c t + \theta_{s,k}) \tag{3}$$

where P_k is the DS-SS signal power, $d_k(t)$ is the data modulation, $c_k(t)$ is the signal spreading code, ω_c is the radian carrier frequency, and $\theta_{s,k}$ is the signal phase, assumed without loss of generality to be zero for convenience in our coherent receiver. The data waveform is of the same form as the MLS data waveform

$$d_k(t) = \sum_i d_i^{(k)} p_T(t - iT) \tag{4}$$

where $d_i^{(k)}$ is the i^{th} bit of user k, in $\{\pm 1\}$, and T is DS-SS bit duration. The spreading signal is of a form similar to (4):

$$c_k(t) = \sum_{n=0}^{N-1} c_{k,n} p_{T_c}(t - nT_c) \tag{5}$$

with the n^{th} chip of the spreading code given by $c_{k,n} \in \{\pm 1\}$, T_c is the chip duration, equal to $1/R_c$, with R_c the chip rate, and the processing gain is $N = T/T_c$. For the spreading signal with pulse shape filtering, we employ the notation $\tilde{c}_k(t)$, about which more will be said subsequently.

Most cellular systems employ "composite codes," which are constructed as the chip-by-chip product of two or more constituent codes. For channelization (user separation) in the GA channel, the use of orthogonal, typically Walsh-Hadamard (WH), codes,[16] would be most suitable. Since the performance of these codes alone is not generally

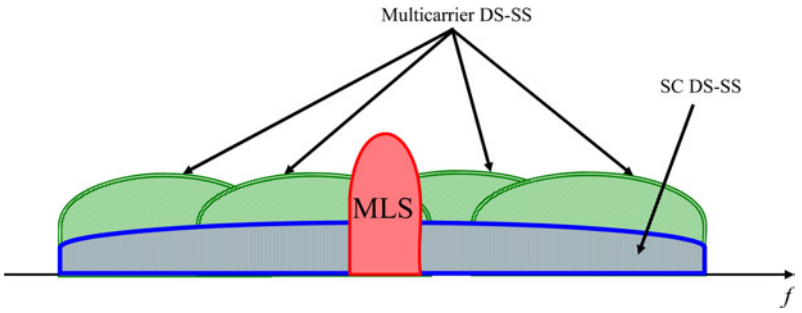

Fig. 2 Illustration of power spectra of MLS and DS-SS signals in overlay mode. [From paper in *Proc. IEEE Aerospace Conf.* (March 6–13, 2004), © 2004 IEEE, Reprinted with permission.]

good in the presence of filtering and channel dispersion,[17] and the code set itself yields unequal amounts of spectrum spreading dependent upon WH code index, a "long" code—whose period is much longer than a single bit—is also used in combination with the WH codes to improve performance and spectral properties. This is what is done in current CDMA cellular systems,[18] and is also planned for future systems.[19,20] Hence, (5) represents a length-N WH code multiplied by a length-N subsequence of a much longer pseudo-random (PR) sequence. These long codes are well-modeled by random Bernoulli sequences.[12] When there are K simultaneous DS-SS-CDMA signals transmitted, the total GA transmitted signal is a sum of terms of the form of (3):

$$s_{DS}(t) = \sum_{k=1}^{K} s_k(t) = \sum_{k=1}^{K} \sqrt{2P_k} d_k(t) c_k(t) \cos(\omega_c t + \theta_{s,k}). \tag{6}$$

As noted, since all K user signals are generated at the same location and can easily be made synchronous, this allows employment of orthogonal spreading codes, most typically the Walsh-Hadamard codes.[16] In practice, these K signals are not perfectly orthogonal after pulse-shape filtering, but the multiuser interference (MUI) that results is minimal—typically 15–20 dB or more below that of the desired signal.[21]

To successfully apply spectral overlay, the DS-SS bandwidth must be much larger than that of the MLS signal. This applies even for multi-carrier systems in which the DS-SS subcarrier bandwidth will be smaller. For the DS-SS systems, this bandwidth is proportional to the chip rate R_c. In Fig. 2 we illustrate conceptually the power spectra of a single-carrier and a multicarrier DS-SS signal and the MLS signal in an overlay mode.

III. Analysis

A. Single Carrier DS-SS Performance

We first quantify the effect of the MLS signal on DS-SS performance. In order to calculate the bit error probability P_b (or bit error ratio, BER) for the DS-SS system, it is necessary to first calculate the statistics of the output of the DS-SS receiver. Figure 3 shows a block diagram of the DS-SS receiver for an arbitrary k^{th} user. In Fig. 3, $w(t)$ is the

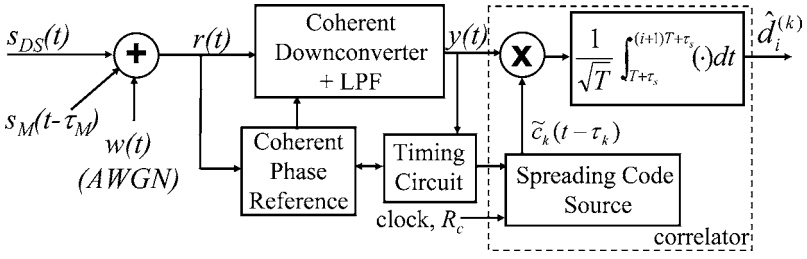

Fig. 3 Block diagram of a DS-SS receiver.

AWGN. This figure shows a conventional correlator receiver, with output $\hat{d}_i^{(k)}$ for user k's i^{th} bit. This output consists of the desired signal term, the MLS interference term, MUI, and AWGN.

When the processing gain N of the DS-SS signal is large, the effects of the MLS signal and the MUI can be modeled as additive Gaussian disturbances to the desired signal. With this Gaussian approximation, we can obtain the probability of bit error for user k, $P_{b,k}$, in closed-form using standard functions. The bit error probability is for most cases equivalent to the BER. With our Gaussian approximation, we have:

$$P_{b,k} = Q(\sqrt{SNIR_k}) = Q\left(\sqrt{\frac{S_k}{P_{N,k} + I_{MLS,k} + I_{0,k}}}\right) \tag{7}$$

where S_k is the square of the mean value of the correlator output $\hat{d}_i^{(k)}$, conditioned on either $a+1$ or -1 sent, and is equal to $E_{bk}T/2$. The term $P_{N,k}$ is the variance of the AWGN part, equal to $N_0T/4$ (independent of k), $I_{MLS,k}$ is the variance of the MLS signal part, and $I_{0,k}$ is the residual multiuser interference density seen by user k, due to the presence of the $K-1$ other DS-SS users, which can be expressed by

$$I_{0,k} = \frac{T}{2}\sum_{\substack{j=1 \\ j\neq k}}^{K} E_{bj}\beta_{kj} \tag{8}$$

where the quantity β_{kj} represents the relative amount of MUI that user k incurs, attributable to user j. This MUI is caused by the non-orthogonality imposed by pulse-shape filtering (in general, this factor could also contain dispersive channel effects that degrade orthogonality as well). We call the term β_{kj} the "MUI factor." It can easily be shown to equal the square of the cross-correlation between user k and user j's spreading codes in the presence of filtering. As an example, if the MUI factor is 15 dB down, $\beta_{kj} = 10^{-15/10} \cong 0.032$. If all DS-SS user transmissions have equal power, and the MUI factors are approximated (or bounded) by a single value β, (8) simplifies to $I_{0,k} \cong \beta T(K-1)E_b/2$.

We use the abbreviation SNIR for the signal-to-noise-plus-interference ratio. The function $Q(x)$ is the tail integral of the zero-mean, unit-variance Gaussian probability density function, equal to $Q(x) = \int_x^\infty e^{-t^2/2}/\sqrt{2\pi}\,dt$. For coherent single-user BPSK in AWGN only, the "I" quantities in (7) are zero.

The performance analysis entails determining the variance of the correlator output $\hat{d}_i^{(k)}$ due to the MLS signal of (1), and selecting parameter values for the MUI factor computation. The means of the MLS and MUI parts of $\hat{d}_i^{(k)}$ are zero when the spreading code is zero mean and/or the MLS and DS-SS data bits are zero mean. We express $\hat{d}_i^{(k)}$ as

$$\hat{d}_i^{(k)} = Ad_i^{(k)} + n_i + m_i + v_i \tag{9}$$

where $d_i^{(k)}$ is DS-SS user k's i^{th} DS-SS data bit, n_i is the noise sample, zero mean with variance $N_0T/4$, m_i is the MLS component of the correlator output, and v_i is the MUI component of the correlator output, which as noted has zero mean, and variance given by (8). We have not used the superscript "k" on the interfering terms of (9) for brevity, and also because with our random spreading code assumption, the statistics for all these terms will be (essentially) invariant to the choice of DS-SS user index. In (9), A is an amplitude, equal to $\sqrt{E_{bk}T/2}$. For the MUI term, specifically, we have

$$v_i = \sqrt{\frac{T}{2}}\sum_{\substack{j=1 \\ j\neq k}}^{K} d_i^{(j)}\sqrt{E_{bj}}\rho_{kj} \tag{10}$$

where the cross-correlation between user k and user j's spreading codes (which is also a function of bit index i by virtue of the use of long PR codes), is given by

$$\rho_{kj} = \int_0^T \tilde{c}_k(t)\tilde{c}_j(t)dt \tag{11}$$

where the function $\tilde{c}_k(t) = c_k(t) * h_T(t)$, $h_T(t)$ is the transmitter pulse shape filter, and the asterisk denotes convolution. In most systems, the receiver pulse shape filter is matched to that of the transmit filter, and is nearly universally

the square-root raised cosine function.[16] If rectangular pulses are used ($h_T(t) = \delta(t)$), the cross-correlation of (11) is identically zero.

In general, the data rates for the DS-SS and MLS signals will not be equal, i.e., $R_{bM} \neq R_b$. It can easily be shown that, for random spreading codes, as long as the chip rate R_c of the DS-SS signal is much greater than R_{bM} (e.g., a factor of 10 or more), the worst-case and average variances of the MLS output of the correlator, and hence the worst-case and average DS-SS P_b performance, will be the same whether $R_{bM} \leq R_b$, or $R_{bM} \geq R_b$. We assume that $R_{bM} \leq R_b$ henceforth in the analysis.

From the perspective of the DS-SS receiver, there are several MLS signal parameters to consider. These include the amplitude, relative delay, and phase of the MLS signal with respect to the DS-SS signal. For analysis, without loss of generality, we consider the DS-SS phase $\theta_{s,k}$ and delay τ_k to be zero, and focus on the zero$^{\text{th}}$ DS-SS bit $d_0^{(k)}$. As noted, the worst-case condition for the DS-SS signal will be when both the MLS frequency f_{cM} and phase θ are identical to those of the DS-SS signal. In addition, the worst-case delay is $\tau_M = iT$, i.e., when the MLS data signal is time-aligned with one of the bit transition times of the DS-SS signal. We derive the MLS variance for the most general case, then specify the result for various values of delay, amplitude, and phase.

From Fig. 3, and (1) and (2), we can obtain the following expression for m_0 of (9), abbreviated hereafter simply as m:

$$\begin{aligned} m &= \sqrt{\frac{E_M}{2T_M}} \int_0^T d_M(t-\tau)\cos(2\pi\,\Delta f t + \theta)\tilde{c}_k(t)dt \\ &= A_m \left\{ \int_0^\tau d_{M,0}\tilde{c}_k(t)\cos(2\pi\,\Delta f t + \theta)dt + \int_\tau^T d_{M,1}\tilde{c}_k(t)\cos(2\pi\,\Delta f t + \theta)dt \right\} \\ &= A_m\{I_1 + I_2\} \end{aligned} \tag{12}$$

where we have abbreviated the constant amplitude term by A_m, the delay τ_M by τ, and $\Delta f = f_c - f_{c,M}$. Since $R_{bM} \leq R_b$, m contains the effect of at most two MLS data bits. We next express the two integrals of (12), I_1 and I_2, by making use of the rectangular pulse shape of the chips of $c_k(t)$. To be precise, the value of the variance of (12) is upper bounded by the value obtained when we use perfect rectangular chip pulses, i.e., when $\tilde{c}_k(t) = c_k(t)$. Use of this as an approximation allows for simpler resulting analysis. Thus, henceforth in our examination of (12), we assume use of $\tilde{c}_k(t) = c_k(t)$. We also assume that the delay τ is random, and by letting $\tau = (q+\varepsilon)T_c$, where q is an integer from 0 to $N-1$, and ε is a real number between 0 and 1, we obtain

$$I_1 = d_{M,0}\left[\sum_{i=0}^{q-2} c_{k,i}\int_{iT_c}^{(i+1)T_c}\cos(2\pi\,\Delta f t + \theta)dt + c_{k,q-1}\int_{(q-1)T_c}^{(q-1+\varepsilon)T_c}\cos(2\pi\,\Delta f t + \theta)dt\right]. \tag{13}$$

Equation (13) simplifies, after completing the integrals, and via trigonometric identities and some algebra, to

$$\begin{aligned} I_1 = d_{M,0}T_c\Bigg[&\frac{\sin(\pi\,\Delta f T_c)}{\pi\,\Delta f T_c}\sum_{i=0}^{q-2} c_{k,i}\cos(\pi\,\Delta f T_c(2i+1)+\theta) \\ &+ c_{k,q-1}\frac{\sin(\pi\,\Delta f \varepsilon T_c)}{\pi\,\Delta f T_c}\cos(\pi\,\Delta f T_c(2q-2+\varepsilon)+\theta)\Bigg]. \end{aligned} \tag{14}$$

Likewise, the second integral is of similar form:

$$\begin{aligned} I_2 = d_{M,1}T_c\Bigg[&\frac{\sin(\pi\,\Delta f T_c)}{\pi\,\Delta f T_c}\sum_{i=q}^{N-1} c_{k,i}\cos(\pi\,\Delta f T_c(2i+1)+\theta) \\ &+ c_{k,q-1}\frac{\sin(\pi\,\Delta f (1-\varepsilon) T_c)}{\pi\,\Delta f T_c}\cos(\pi\,\Delta f T_c(2q-1+\varepsilon)+\theta)\Bigg]. \end{aligned} \tag{15}$$

As noted, the mean of m is 0 by virtue of the zero-mean MLS data bits and the zero-mean code chips. The variance of m, σ_m^2 (= $I_{MLS,k}$ of (7)), is thus equal to its mean-square value $E[m^2]$. The expectation of the product $I_1 I_2$ is zero via independence of the data bits, so $\sigma_m^2 = E[m^2]$ is equal to the sum of the expectations of the squares of (14) and (15). After minor algebraic simplification, we obtain:

$$\sigma_m^2 = \frac{E_M T_c^2}{2T_M} \left\{ \frac{\sin^2(\pi \Delta f T_c)}{(\pi \Delta f T_c)^2} \sum_{\substack{i=0 \\ i \neq q-1}}^{N-1} \cos^2[\pi \Delta f T_c (2i+1) + \theta] \right.$$
$$+ \frac{\sin^2(\pi \Delta \varepsilon f T_c)}{(\pi \Delta f T_c)^2} \cos^2[\pi \Delta f T_c (2q - 2 + \varepsilon) + \theta]$$
$$\left. + \frac{\sin^2(\pi \Delta (1-\varepsilon) f T_c)}{(\pi \Delta f T_c)^2} \cos^2[\pi \Delta f T_c (2q - 1 + \varepsilon) + \theta] \right\} \tag{16}$$

Equation (16) can be used to evaluate the variance of the MLS interference term for any arbitrary value of MLS signal power, carrier frequency, relative delay, and carrier phase. Often we are interested in averages over some or all of these parameters. For example, if we average (16) over the carrier phase θ, we obtain

$$\sigma_m^2 = \frac{E_M T_c^2}{2T_M} \left\{ \frac{\sin^2(\pi \Delta f T_c)}{(\pi \Delta f T_c)^2} \frac{(N-1)}{2} + \frac{1 - \cos(\pi \Delta f T_c) \cos[\pi \Delta f T_c (1 - 2\varepsilon)]}{2(\pi \Delta f T_c)^2} \right\}, \tag{17}$$

which turns out to be independent of the integer part (q) of the delay τ. In addition, we are also interested in worst-case values. The maximum value of σ_m^2 occurs when $\Delta f = 0, \theta = 0$, and $\tau = 0$, for which we obtain the simple form $\sigma_m^2 = (N E_M T_c^2)/(2T_M)$. Other cases are also of interest. In Table 1 we list values of the MLS variance term for various cases. Two of these results are described below the table.

In Table 1, the term "Avg"=averaged means that we have averaged over the distribution of the random variable in question, all of which are uniform, i.e., $\tau \sim U(0, T)$, which implies q is a uniformly distributed integer from 0 to $N-1$ and ε is a continuous uniform random variable from 0 to 1, and $\theta \sim U[0, 2\pi)$. The term "Arb" = arbitrary value. The result for the case when the MLS signal center frequency is at the first spectral null of the DS-SS signal

Table 1 MLS Component Signal Variance for Various Cases. [From paper in *Proc. IEEE Aerospace Conf.* (March 6–13, 2004), © 2004 IEEE, Reprinted with permission.]

Δf	τ	θ	σ_m^2	Comments
0	0	0	$\frac{N E_M T_c^2}{2T_M}$	Worst-case
0	Avg	0	$\frac{(N - 1/3) E_M T_c^2}{2T_M}$	—
0	Avg	Avg	$\frac{(N - 1/3) E_M T_c^2}{4T_M}$	—
Arb	Arb	Arb	Eq. (16)	Most general formula
Arb	Arb	Avg	Eq. (17)	—
$\pm R_c$	Arb	Arb	Eq. (18)	MLS signal in DS-SS first null; upper bounded by $\frac{E_M T_c^2}{\pi^2 T_M}$
Arb	Avg	Avg	Eq. (19)	Averaged over delay and phase

($\Delta f = \pm R_c$) is given by

$$\sigma_m^2 = \frac{E_M T_c^2}{2T_M}\left\{\frac{\sin^2(\pi\varepsilon)}{\pi^2}\cos^2[\pi(2q-2+\varepsilon)+\theta] + \frac{\sin^2(\pi(1-\varepsilon))}{\pi^2}\cos^2[\pi(2q-1+\varepsilon)+\theta]\right\} \tag{18}$$

for which an upper bound is given in Table 1. The result for the average over all parameters (except frequency) is the most complicated expression:

$$\sigma_m^2 = \frac{E_M T_c^2}{2T_M}\left\{\frac{\sin^2(\pi\,\Delta f T_c)}{(\pi\,\Delta f T_c)^2}A + \frac{1-\sin(2\pi\,\Delta f T_c)/(2\pi\,\Delta f T_c)}{2(\pi\,\Delta f T_c)^2} + \frac{\sin(2\pi\,\Delta f N T_c)/(2\pi\,\Delta f T_c)}{4\,N(\pi\,\Delta f T_c)^2\sin(2\pi\,\Delta f T_c)}[B+C+D]\right\} \tag{19}$$

where the terms *A, B, C*, and *D* of (19) are given as follows:

$$A = \frac{N-1}{2} + \frac{\cos(2\pi\,\Delta f N T_c+\theta)\sin(2\pi\,\Delta f N T_c)}{2\sin(2\pi\,\Delta f T_c)} - \frac{\cos(2\pi\,\Delta f T_c(N-2)+2\theta)\sin(2\pi\,\Delta f N T_c)}{2N\sin(2\pi\,\Delta f T_c)} \tag{20}$$

$$B = \frac{\sin(\pi\,\Delta f T_c)}{\pi\,\Delta f T_c}[2\cos(2\pi\,\Delta f T_c(N-4)+2\theta)\sin(2\pi\,\Delta f T_c)] \tag{21}$$

$$C = \frac{\sin(2\pi\,\Delta f T_c)}{4\pi\,\Delta f T_c}\{\cos[2\pi\,\Delta f T_c(N-2)+2\theta]\}\times(1+\cos(2\pi\,\Delta f T_c(N-1)+2\theta)) \tag{22}$$

$$D = \frac{-\sin(2\pi\,\Delta f T_c)}{4\pi\,\Delta f T_c}\{\cos[2\pi\,\Delta f T_c(N-3)+2\theta]\} \tag{23}$$

The results of (18) and (19) can be shown to reduce to the others in Tab. 1 for the appropriate parameter settings. Using these expressions allows evaluation of the DS-SS error probability in the presence of the MLS signal. Specifically, we have

$$P_{b,k} = Q\left(\sqrt{\frac{2E_b}{N_0 + 4\sigma_m^2/T + I_{0,k}}}\right) \tag{24}$$

where $I_{0,k}$ is given by (8). We use (24) to evaluate the DS-SS performance in the section on numerical results.

B. Multicarrier DS-SS Performance

For this case, we can make use of all the results of the previous section. For most cases, we will still have $R_c >> R_{bM}$, so that all the assumptions made for the single-carrier case still apply. The main difference in performance arises because *not* all the subcarriers of the MC-DS-SS signal will be affected by the narrowband MLS signal. Thus, we can use (24), with the appropriate value of R_c and powers, to evaluate the performance of a *single* subcarrier. For a fair comparison, we require that the total bandwidths and data rates of the multicarrier systems are equal to that of the single carrier system. By equating these, we obtain equations for the processing gains of each. Depending upon the way the DS-SS data bits are distributed across the subcarriers, we obtain two different cases. In both of these cases, we neglect the presence of additional CDMA users for simplicity. Accounting for them would be done in a manner analogous to that for the SC DS-CDMA case.

Case 1: Serial to Parallel Conversion—For this case, independent data bits are distributed across the M subcarriers, so only a fraction $1/M$ bits are affected by the interference, since the MLS signal will affect primarily a single subcarrier. The symbol rate R_s on each subcarrier is equal to the bit rate R_b divided by M, and the energy of each symbol is E_b. Hence, the bit error probability expression is

$$P_b = \frac{M-1}{M}P_{bA} + \frac{1}{M}P_{bI} \tag{25}$$

where P_{bA} is the performance of the modulation in AWGN, and P_{bI} is the performance in the presence of the MLS interference. For BPSK, $P_{bA} = Q(\sqrt{2E_b/N_0})$, and P_{bI} is obtained via (24) with the appropriate values for the parameters of the MLS signal, and the single affected subcarrier of the MC-DS-SS signal.

For equal (3 dB) bandwidths and data rates (and BPSK modulation), we can show that the processing gain of this MC case, N_{MC1}, is equal to that of the single carrier case, N. The bandwidth of the single carrier case is approximately NR_b, and that of the multicarrier case is similarly $N_{MC1}R_b$. The chip rate of this multicarrier case, $R_{c,MC1}$, is equal to the single-carrier chip rate R_c divided by the number of subcarriers M. Thus, for example, P_{bI} of (25) for the worst-case condition ($\Delta f = \tau = \theta = 0$), is obtained as

$$P_{bIwc} = Q\left(\sqrt{\frac{2E_b/N_0}{1 + 2(P_M/P)(E_b/N_0)(M/N_{MC1})}}\right). \tag{26}$$

Case 2: Splitting—For this case, each data bit of the DS-SS signal has $(1/M)^{th}$ of its *energy* distributed across each of the M subcarriers, so $E_{bi} = E_b/M$ for subcarrier i, and $R_{bi} = R_b$. This is the system considered in,[13] which can achieve frequency diversity across the M subcarriers. At the receiver, the correlator outputs of the M correlators are added together before making a bit decision. As with the single carrier version, we condition upon a $+1$ being sent, and obtain the mean and variance of the summed output. The mean is the sum of the M outputs, each of which has a mean of $\sqrt{E_bT/(2M)}$, so the composite decision variable mean is $\sqrt{ME_bT/2}$. The variance of the decision variable is the sum of the "noise" variances on each subcarrier, equal to $(MN_0T/4) + \sigma_m^2$, hence we have

$$P_b = Q\left(\sqrt{\frac{2E_b}{N_0 + 4\sigma_m^2/(MT)}}\right). \tag{27}$$

For equal (3 dB) bandwidths and data rates (and BPSK modulation), we can show that the processing gain of this second MC case, N_{MC2}, is equal to that of the single carrier case, N, divided by M. The bandwidth of the single carrier case is approximately NR_b, and that of this second multicarrier case is $N_{MC2}MR_b$. The chip rate of this multicarrier case, $R_{c,MC2}$, is also equal to the single-carrier chip rate R_c divided by the number of subcarriers M. For the worst-case condition ($\Delta f = \tau = \theta = 0$), (27) becomes

$$P_b = Q\left(\sqrt{\frac{2E_b/N_0}{1 + (2(P_M/P)(E_b/N_0)/(MN_{MC2}))}}\right) \tag{28}$$

For this particular case, the MC error probability is *identical* to that of the equivalent single carrier DS-SS system.

C. MLS Performance

For all cases, we assume that the DS-SS bandwidth is much larger than that of the MLS signal. We model the DS-SS interference as an additive white Gaussian disturbance imposed at the MLS receiver, and determine the error probability of the MLS digital signal. Although error probability may not be the best measure of performance for the MLS system, the SNIR expression used in determining BER is certainly applicable—we employ the BER measure for simplicity and insight. In the error probability expression for the MLS signal, we add an additional Gaussian term to the thermal noise term. This DS-SS interference correlator output term is $PT_M/(2R_c)$. This approximation for the DS interference is very good for DS-SS bandwidths as small as a few times B_{MLS}. After some algebra we obtain

$$P_{b,M} = Q\left(\sqrt{\frac{2E_{b,M}}{N_0 + 2P_{T,DS}/R_c}}\right) \tag{29}$$

where now $P_{T,DS}$ is the *total* DS-SS signal power, equal to KP if all DS-SS user signals are transmitted with power P. We note that the expression of (29) actually applies to the differentially-encoded bits ($d_{M,k}$ in (2)). When these error probabilities are near 0.01 or smaller, the actual bit error probability of the data bits (b_k) is very well approximated by twice the value in (29).[12] When we employ the power ratio $P_{T,DS}/P_M$, via simple algebraic manipulations, we can express (29) as

$$P_{b,M} = Q\left(\sqrt{\frac{2E_{b,M}/N_0}{1 + 2(P_{T,DS}/P_M)(E_{b,M}/N_0)(R_{bM}/R_b)/N}}\right) \tag{30}$$

which illustrates directly the effect of the different system data rates and DS-SS processing gain N.

D. DS-SS CDMA Capacity

From the MLS BER expressions, we can determine a reasonable value for the ratio of received DS-SS to MLS signal powers such that the MLS performance is minimally degraded (we illustrate this in the next section). Given that we can determine such a value P_{DS}/P_M, we can employ this in the BER expression for DS-SS to estimate the supportable number of DS-SS-CDMA users K for a given desired BER. Specifically, we employ only the worst-case DS-SS-CDMA expression, Eq. (24), with the MLS variance σ_m^2 equal to $NE_M T_c^2/(2T_M)$, (which, again, assumes $\Delta f = \tau = \theta = 0$). We also use the MUI approximation that employs a single MUI factor β. Using these in (24), and setting the argument of the resulting Q-function equal to that required for a desired DS-SS-CDMA BER, we can solve for the maximum number of CDMA users K. After some algebra we obtain the following:

$$K \leq \frac{2\gamma - \psi + 2\psi\beta\gamma}{\psi\left(2P_M/(P_{T,DS})(\gamma/N) + 2\beta\gamma\right)}. \tag{31}$$

where $\gamma = E_b/N_0$, the SNR per bit of the DS-SS system, determined from link budget parameters, and ψ is the value in the expression $Q(\sqrt{\psi}) = P_{b,DS}$ required to obtain the desired DS-SS BER value $P_{b,DS}$; for example, for $P_{b,DS} = 10^{-3}$, $\psi \cong 9$, and for $P_{b,DS} = 10^{-2}$, $\psi \cong 5$.

IV. Numerical Results

We have computed the DS-SS P_b according to (24) for several cases, to gain insight into the range of feasible values of several signal parameters. We have also developed computer simulations to corroborate the analytical results of the previous section. These simulations were conducted in MATLAB. Parameters we vary are the DS-SS processing gain N, the signal-to-noise (only) ratio, expressed as E_b/N_0, the MUI factor β, and the ratio of the received MLS signal power to the received DS-SS signal power, expressed as the jamming-to-signal-ratio (JSR). In most of the numerical results we choose a DS-SS chip rate of $R_c = 30$ MHz, which is approximately half the bandwidth of the MLS allocation (5091–5150 MHz), allowing for an FDD AG channel.

Figure 4 shows P_b as a function of SNR for several different values of MLS signal power to DS-SS signal power, abbreviated the jamming-to-signal power ratio, JSR. We have used the worst-case P_b expressions (Table 1). In Fig. 4,

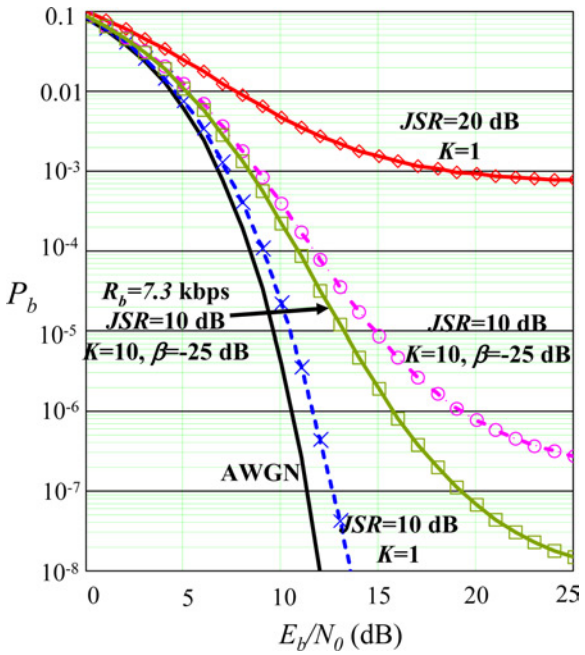

Fig. 4 DS-SS worst-case P_b vs. E_b/N_0 with $R_c = 30$ MHz, several values for JSR and number of DS-SS users K.

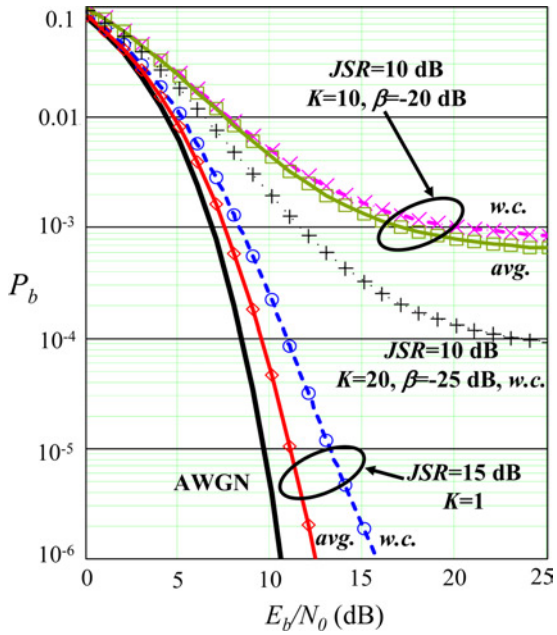

Fig. 5 DS-SS P_b vs. E_b/N_0 with $R_c = 30$ MHz, $R_b = 29.3$ kbps, several values of JSR and number of DS-SS users K, and worst-case (w.c.), average (avg.) values of delay τ and phase θ.

the chip rate of the DS-SS system is 30 MHz, and the bit rate of the DS-SS system for all but one of the curves is 29.3 kbps; for one curve we use $R_b = 7.3$ kbps. These values result in processing gains of 1024 or 4096. We have used a value of -25 dB for the MUI factor β. If for example the DS-SS system requires an error probability of no greater than 10^{-3}, and an E_b/N_0 of 10 dB can be maintained, the acceptable JSR is approximately 10 dB for up to 10 DS-SS-CDMA users at these bit rates. These values can be translated, via link budget equations, into acceptable transmit power levels and ranges.

In Fig. 5, a plot similar to Fig. 4 is shown. In this case, the chip rate of the DS-SS system is again 30 MHz, and the bit rate 29.3 kbps. We show the difference between the worst-case performance and performance when averaged over the MLS random delay τ and phase θ. Performance can clearly be a strong function of these parameters. We also show how the number of DS-SS-CDMA users varies with both the JSR and the MUI factor, illustrating the importance of the choice of pulse shape filter for the DS-SS-CDMA system.

In Fig. 6 we show DS-SS performance again for $R_c = 30$ MHz and $R_b = 29.3$ kbps, but here the MLS signal is centered not on the DS-SS spectrum, but at its first spectral null, i.e., $\Delta f = \pm R_c$, so the upper bound on (18) is employed. In this case we show that generally, the DS-SS system can support a larger number of users, as expected. Worth noting is that in this case with $\Delta f = \pm R_c$, the MLS signal could also affect the adjacent frequency AG channel, so investigation of that link's capacity would be simultaneously required for this frequency arrangement.

Figure 7 shows a comparison of simulation and analytical results for two values of the JSR (J/S). We have simulated the worst-case DS-SS conditions, where $\Delta f = \tau = \theta = 0$, and with a single DS-SS user, for simplicity. As can be seen, agreement between analysis and simulations is excellent. The simulations were conducted in MATLAB, and at least 100 errors were counted at each value of the error probability. For this case, the simulations and analysis validate one another—the additional utility of simulations is the study of performance for cases where analysis is intractable.

Another question of interest in these spectral overlay systems is the achievable data rate for a given set of system parameters. Figure 8 shows the achievable bit rate for a DS-SS system in the presence of the MLS interference; the bit rate is plotted as a function of distance between the DS-SS receiver and DS-SS transmitter (i.e., communication link range). Three desired values for P_b are assumed for the DS-SS system, which translate into fixed values for the DS-SS SNIR of (24). It is also assumed that the distance between the DS-SS receiver and DS-SS transmitter

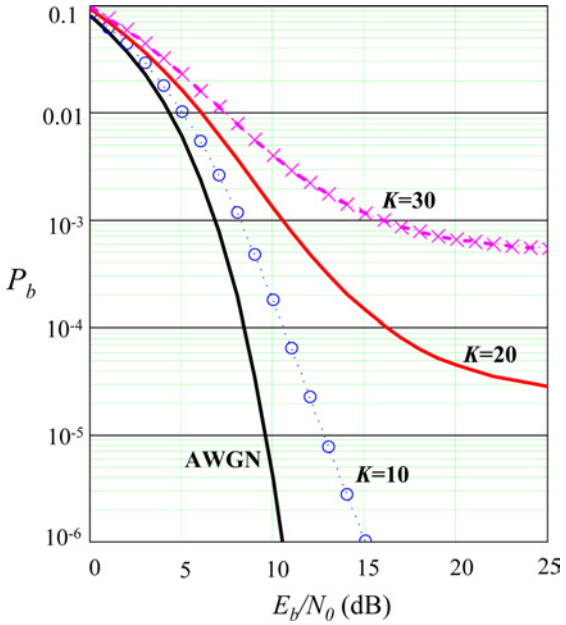

Fig. 6 DS-SS P_b vs. E_b/N_0 with $R_c = 30$ MHz, $R_b = 29.3$ kbps, $JSR = 10$ dB, $\beta = -25$ dB, and $\Delta f = \pm R_c$, for several values of the number of DS-SS-CDMA users K.

is identical to that between the MLS transmitter and MLS receiver, or in other words, the DS-SS and MLS ground transmitters are close compared to the link range. In addition, we assume that both the MLS and DS-SS transmitters transmit only one watt of power. Finally, a chip rate of 20 MHz, and a single DS-SS user were assumed for the DS-SS system. Figure 8 was obtained numerically, based upon simple link equations, in which all antenna gains are zero dB (which is likely pessimistic for the DS-SS system), and the channel attenuation is modeled as that of free space. Worth noting is the fact that these results apply to uncoded modulation—actual error probabilities would be significantly

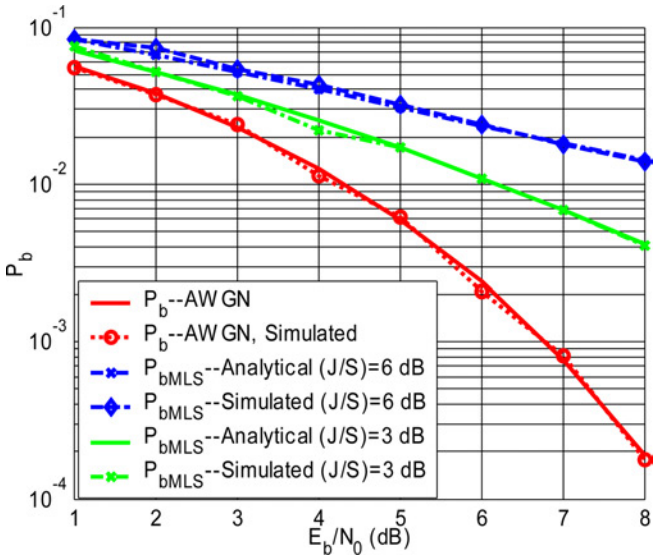

Fig. 7 Comparison of analytical and simulation results for DS-SS P_b vs. E_b/N_0 with MLS interference. [From paper in *Proc. IEEE Aerospace Conf.* (March 6–13, 2004), © 2004 IEEE, Reprinted with permission.]

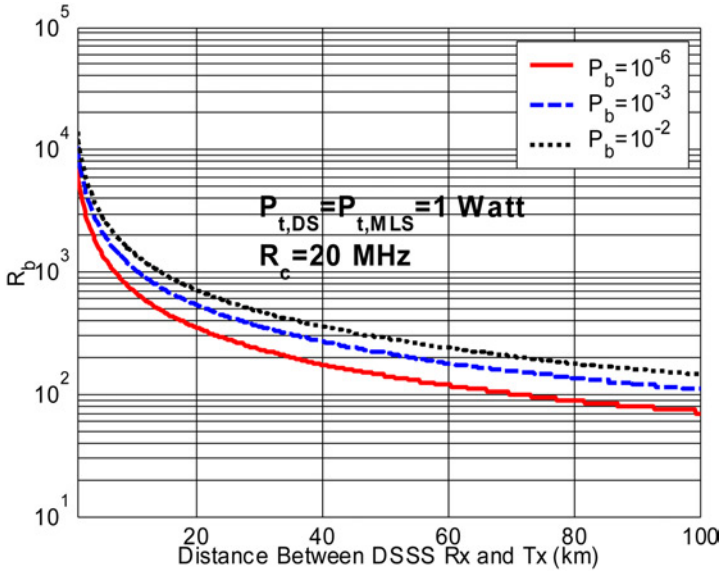

Fig. 8 Achievable (uncoded) DS-SS data rate R_b (bps) for given P_b vs. link range, in presence of MLS. [From paper in *Proc. IEEE Aerospace Conf.* (March 6–13, 2004), © 2004 IEEE, Reprinted with permission.]

lower with forward error correction (FEC), which would be used in any practical system. Thus, the achievable data rates in our example are significantly lower than those attainable in practice with higher power antennas, higher gain antennas, and FEC.

For assessing the degradation incurred by the MLS system in the presence of the DS-SS signal, we employ (30). As a simple example we show in Fig. 9 the achievable MLS $P_{b,M}$ versus E_{bM}/N_0, for several JSR values, where here, JSR is the ratio of DS-SS signal power to MLS signal power. Again these are worst-case values, with the DS-SS center frequency equal to that of the MLS signal. The chip rate of the DS-SS signal is again the 30 MHz value

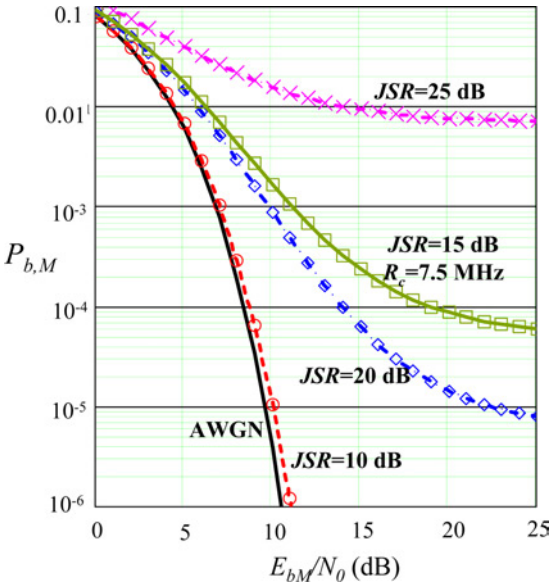

Fig. 9 MLS P_b vs. E_b/N_0, with $R_c = 30$ or 7.5 MHz, $R_b = 29.3$ or 7.3 kbps, respectively, for various JSR values.

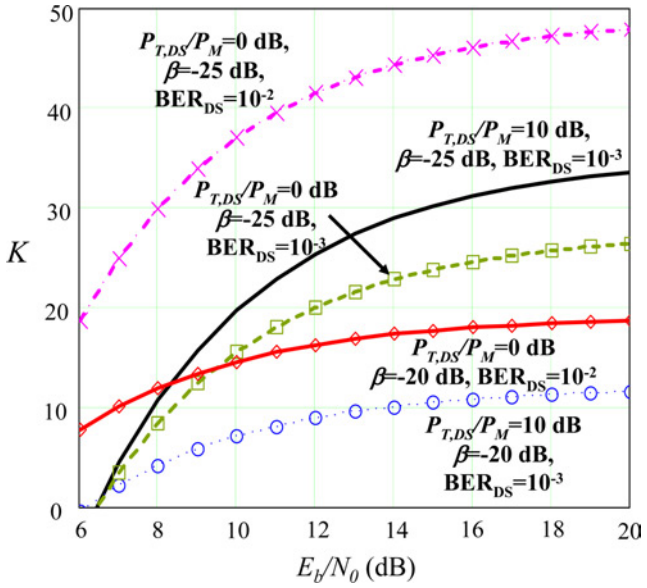

Fig. 10 Supportable number of DS-SS-CDMA users K vs. DS-SS-CDMA E_b/N_0, with several values of JSR ($P_{T,DS}/P_M$), MUI factor β, and required DS-SS-CDMA BER$_{DS}$.

assumed previously, with DS-SS bit rate of 29.3 kbps, and we also show performance for both chip rate and data rate reduced by a factor of four, i.e., $R_c = 7.5$ MHz, and $R_b \cong 7.3$ kbps. Clearly when the ratio of DS-SS to MLS power is not too large (JSR ≤ 10 dB), the MLS system suffers very little from the presence of the wideband DS-SS signal(s).

Finally, as per our discussion in Section III.D, we illustrate in Fig. 10 the supportable number of users in the DS-SS-CDMA system K vs. the DS-SS received SNR per bit E_b/N_0 (this is the thermal SNR per bit only). This figure assumes several values for the MUI factor β, a DS-SS processing gain $N = R_c/R_b = 1024$, corresponding again to $R_c = 30$ MHz and $R_b = 29.3$ kbps, two values of MLS JSR $P_{T,DS}/P_M$, and two different required values of CDMA BER, 10^{-2} and 10^{-3}. From Fig. 9 we note that for these chip and data rates, the MLS performance does not appreciably degrade when the MLS JSR $P_{T,DS}/P_M \leq 10$, so with this fact, Fig. 10 illustrates the tradeoff between the MUI factor β, JSR, and required CDMA BER. For examples, referring to the lower two curves in Fig. 10, if the required CDMA BER is 10^{-3}, the MUI factor $\beta = -20$ dB, and the JSR $P_{T,DS}/P_M$ is 10 (=10 dB), approximately $K = 10$ CDMA users can be supported, requiring an $E_b/N_0 \geq 14$ dB. The E_b/N_0 requirement directly translates into link budget parameters. If the CDMA BER requirement is relaxed to 10^{-2}, with the same value of β a lower JSR $P_{T,DS}/P_M = 1$ (0 dB) and larger number of DS-SS-CDMA users (approximately 18) can be supported. We note again that these BER values are *before* FEC decoding, which would reduce the final CDMA user BER by several orders of magnitude.

V. Summary and Conclusions

In this paper, we have explored the feasibility of the use of spectral overlay of DS-SS in the MLS band via use of classical analytical techniques and a first-order model for the channel. We developed expressions for the error probability performance of DS-SS in the presence of MLS (digital) interference and (synchronous) multiuser DS-SS CDMA interference, and for the MLS error probability performance in the presence of DS-SS. We corroborated these analytical results with computer simulations.

We identified the pertinent DS-SS signal parameters necessary for a proper evaluation: the DS-SS processing gain and data rate, the relative transmit power, and the total number of DS-SS users. The MLS signal/system parameters of most importance are the MLS signal power and center frequency with respect to that of the DS-SS signal. Given a

careful system design, and allowing either some small degradation to the MLS error probability, or a slightly reduced MLS range, the use of a DS-SS spectral overlay is feasible. For the most part, multicarrier DS-SS techniques appear to have little if any advantage over the single-carrier technique—implementation issues could affect this observation somewhat, but as long as the single-carrier DS-SS chip rate is not too high (say, less than 50 MHz), the single-carrier DS-SS approach is simpler and implementable with current technology. The MC approaches do offer increased flexibility in spectrum management.

These results are the first of those required for a proper application of spectral overlay in the MLS band, and serve to illustrate the method. Additional work is required to firmly establish the feasibility of this technique, including study of additional overlay applications, such as any used in GPS. This work would begin with obtaining minimally acceptable values of the MLS performance. The use of realistic link ranges would also be needed to estimate potential performance and data rates of the DS-SS system. Other areas of research include the incorporation of spatial effects of the MLS transmission, the use of more accurate channel models, the data link layer design (e.g., burst transmission format), and the potential use of interference cancelling (filtering) of the MLS signal in the DS-SS receiver to improve DS-SS performance, and filtering the DS-SS transmissions (spectral "notching") to improve MLS performance.

References

[1]Department of Transportation, Federal Aviation Administration (FAA) National Airspace System (NAS) website, http://www2.faa.gov/nasarchitecture/blueprnt/comm.htm, 27 June 2003.

[2]Burke, G., "Shaping the National Airspace System for the 21st Century," *Proc. of 16th Digital Avionics Systems Conference*, Irvine, CA, pp. 0.4-1–0.4-7, 26–30 October, 1997.

[3]Smith, P., "IPSKY: IPv6 for the Aeronautical Telecommunications Network," *Proc. of 20th Digital Avionics Systems Conference*, Daytona Beach, FL, pp. 7.A.6-1–7.A.6-11, 14–18 October, 2001.

[4]Martzaklis, K., "NASA Datalink Communications Research & Technology Development For Aeronautics," *Proc. of Integrated CNS Workshop*, Session E—Research and Technology Development for Far-Term Datalink Systems, Cleveland OH, 1–3 May 2001.

[5]Kabaservice, T. P., "Technical and Economic Benefits of VHF Digital Link Mode 3 Integrated Voice and Data Link for Air Traffic Control Communications," *Proc. of Integrated CNS Workshop*, Session B1—Datalink Communication Systems, pp. 55–59, Annapolis, MD, 19–22 May 2003.

[6]Jahn, A., Holzbock, M., Muller, J., Kebel, R., de Sanctis, M., Rogoyski, A., Trachtman, E., Franzrahe, O., Werner, M. and Hu, F., "Evolution of Aeronautical Communications for Personal and Multimedia Services," *IEEE Communications Magazine*, Vol. 41, No. 7, pp. 36–43, July 2003.

[7]Matolak, D. W., "CDMA for Communications in the Aeronautical Environment," *Proc. 16th Digital Avionics Systems Conference*, Irvine, CA, pp. 9.4-21–9.4-28, October 1997.

[8]Haas, E., and Schnell, M., "Advanced Airport Data Link—Concept and Demonstrator Implementation for a Modern Airport Data Link," *Proc. of Integrated CNS Workshop*, Session B1—Datalink Communication Systems, pp. 83–92, Annapolis, MD, 19–22 May 2003.

[9]Milstein, L. B., Schilling, D. L., Pickholtz, R. L., Kullback, M., Kanterakis, E. G., Fishman, D. S., Biederman, W. H., and Salerno, D. C., "On the Feasibility of a CDMA Overlay for Personal Communications Networks," *IEEE Journ. Select. Areas in Comm.*, Vol. 10, pp. 655–668, May 1992.

[10]Matolak, D. W., "On the Overlay of CDMA onto the Aeronautical VHF Band: An Inter-System Interference Analysis," *MITRE Technical Report* 97W0000137, December 1997.

[11]Matolak, D. W., and Neville, J. T., "Spectral Overlay of Direct-Sequence Spread Spectrum in the Instrument Landing System Glideslope Band," *AIAA Journ. of Aerospace Computing, Information, and Communication*, Vol. 1, October 2004.

[12]Peterson, R. L., Ziemer, R. E., and Borth, D. E., *Introduction to Spread Spectrum Communications*, Prentice-Hall, Upper Saddle River, NJ, 1995.

[13]Kondo, S., and Milstein, L. B., "Performance of Multicarrier DS CDMA Systems," *IEEE Trans. Comm.*, Vol. 44, No. 2, pp. 238–246, February 1999.

[14]Helfrick, A., *Principles of Avionics*, 3rd ed., Avionics Communications, Inc., 2004.

[15]DiBenedetto, M. F., *Development of Critical-Area Criteria for Protecting Microwave Landing System Azimuth and Elevation Antenna Guidance Signals*, Ph.D. Dissertation, Ohio University, March 1999.

[16]Viterbi, A. J., *CDMA: Principles of Spread Spectrum Communication*, Addison-Wesley, Reading, MA, 1995.

[17]Schnell, M., "Hadamard Codewords as Orthogonal Spreading Sequences in Synchronous DS CDMA Systems for Mobile Radio Channels," *Proc. 3rd IEEE International Symposium on Spread Spectrum Techniques and Applications*, ISSTA'94, Oulu, Finland, 1994.

[18]TIA/EIA/IS-95-A, "Mobile station-base station compatibility standard for dual-mode wideband spread spectrum cellular system," 1995.

[19]Third Generation Partnership Project (3GPP), world wide web site, http://www.3gpp.org, August 2004.

[20]Third Generation Partnership Project Two (3GPP2), world wide web site, http://www.3gpp2.org, August 2004.

[21]Matolak, D. W., and Roos, M. J., "Computation of the Multi-User Interference due to Pulse Shape Filtering for the IS-95 Forward Channel," *MITRE Technical Report*, October 1997.